Selectively Probing the Glass Transition Temperature in Multilayer Polymer Films: Equivalence of Block Copolymers and Multilayer Films of Different Homopolymers

Connie B. Roth[†] and John M. Torkelson*[,†,‡]

Department of Chemical and Biological Engineering and Department of Materials Science and Engineering, Northwestern University, Evanston, Illinois 60208-3120

Received January 20, 2007; Revised Manuscript Received March 12, 2007

ABSTRACT: The temperature dependence of the fluorescence of trace levels of pyrene was employed to measure the glass transition temperatures (T_gs) of polystyrene (PS) domains within ultrathin films of poly(styrene-*block*-methyl methacrylate) (P(S-*b*-MMA)) and poly(styrene-*block*-2-vinylpyridine) (P(S-*b*-2VP)) diblock copolymers supported on silica after self-assembly into lamellar morphologies. The PS domains within the two block copolymers exhibited dramatically different T_g−nanoconfinement behavior. The T_gs of the PS domains within the P(S-*b*-MMA) films were observed to decrease with decreasing film thickness in accordance with T_g reductions observed for single-layer PS homopolymer films; in contrast, the T_g of the PS domains within the P(S-*b*-2VP) films exhibited no change within experimental uncertainty upon confinement. The T_gs of the block copolymer films showed excellent agreement with those of multilayer films constructed from homopolymer layers with an equivalent morphology, indicating that chain connectivity across the immiscible interface has little impact on cooperative segmental dynamics within the individual layers/domains. The difference in the T_g−nanoconfinement behavior exhibited by the PS free-surface layer of P(S-*b*-MMA) and P(S-*b*-2VP) block copolymer films, and equivalently exhibited by the PS free-surface layer of PS/PMMA and PS/P2VP bilayer films, is due to the much stronger attractive interaction at the P2VP−silica substrate interface. Once the P2VP−silica substrate interaction is removed, the P2VP underlayer is no longer able to suppress the enhanced mobility of a PS free-surface layer when the underlayer thickness is made sufficiently thin ($<\sim$10 nm). This indicates that both the *type* and *amount* of material present in the underlayers determine the T_g−nanoconfinement behavior at the free surface of multilayer films. In addition, intrinsic phenyl ring fluorescence was shown to be effective for quantifying in situ the time scale for self-assembly of styrene-containing block copolymers.

Introduction

With recent advances in polymer processing yielding nanoscale layer or domain sizes,[1−9] there is potential for significant property improvements with important technological applications. For instance, multilayer films of different polymers are used in applications ranging from barrier layers for food packaging[9] to films with unique optical properties.[2] These multilayer films can consist of a few to thousands of layers with each layer having nanoscale thickness.[2−4] With the advent of such systems, it is important to characterize and understand the extent to which the nanoscale size of the domains/layers as well as the many interfacial regions ("interphase") affect the properties of both the overall material and the individual domains/layers.

Research on amorphous materials in confined geometries, especially in polymers in ultrathin films, has demonstrated the large impact that interfaces, both free surfaces and hard interfaces, can have on properties.[10−48] Changes in the glass transition temperature, T_g, of up to tens of kelvin[11−44] and enhanced or suppressed physical aging rates[42−48] have been reported. Three polymers which illustrate the range of effects are polystyrene (PS), poly(2-vinylpyridine) (P2VP), and poly(methyl methacrylate) (PMMA). Nanoconfined PS films supported on silica exhibit a large decrease in T_g with decreasing thickness relative to the bulk value, T_g^{bulk}. This occurs because the free-surface layer of PS exhibits a decrease in T_g resulting from a reduction in the requirement for cooperativity in the segmental mobility associated with T_g.[16] In contrast, the PS−silica interface has little or no effect on T_g because there is no significant attractive interaction between PS and the silica surface.[15] For 15 nm thick PS films supported on silica, $\Delta T_g = T_g - T_g^{bulk} = -30$ K,[11,13,15,16] and the T_g reductions are even larger for free-standing films with two polymer−air interfaces.[22,23] In contrast, P2VP films supported on silica exhibit an increase in T_g with decreasing thickness, with $T_g - T_g^{bulk} = +30$ K for 15 nm thick films.[17−19] With P2VP, the cooperative segmental dynamics are hindered by hydrogen bonds between the nitrogen atom in the repeat unit and hydroxyl groups on the silica surface. A recent study has indicated that the free surface of a supported P2VP film has negligible effect on T_g behavior in comparison with P2VP−silica interface effects.[19] The T_g values of nanoconfined PMMA films supported on silica also increase with decreasing thickness, although to a smaller extent than for P2VP. With PMMA, the attractive interactions at the polymer−substrate interface, involving hydrogen bonds between ester side groups on PMMA and the hydroxyl groups on the substrate surface, apparently have a greater influence on the overall T_g behavior than the free-surface effect, which has been shown with free-standing films to be weaker in PMMA than in PS.[24,25]

Our recent study of PS/P2VP and PS/PMMA bilayer films, which were made by layering spin-coated films atop each other, revealed that the T_g of a PS free-surface layer can be substantially altered by the polymer in the underlayer, indicating that dynamics are coupled across the polymer−polymer interface.[19] The narrow interfacial widths between immiscible polymer layers, reported to be 3.4 and 5.0 nm for PS/P2VP[49]

* To whom correspondence should be addressed: e-mail j-torkelson@northwestern.edu.
[†] Department of Chemical and Biological Engineering.
[‡] Department of Materials Science and Engineering.

10.1021/ma070162g CCC: $37.00
Published on Web 04/07/2007

and PS/PMMA,[50] respectively, result in cooperatively rearranging regions (CRRs) that contain segments from both polymers. In the bilayer study, it was demonstrated that bulk underlayers of both P2VP and PMMA can nearly eliminate the large (∼32 K) T_g reductions typically present in a 14 nm thick PS free-surface layer when supported on bulk PS.[19]

Besides being made by layering spin-coated films, multilayer films can also be formed by coextrusion,[2−4,51] layer-by-layer assembly,[52] or self-assembly from diblock copolymers.[53−62] Here, we choose to compare the behavior of films of diblock copolymers self-assembled into lamellar (and thereby multilayer) morphologies with multilayer films of equivalent morphologies assembled by hand from homopolymer films. We investigate multilayer films in ultrathin film geometries to probe directly the impact of free surface and substrate interactions on the dynamics within the film and to determine the extent to which these effects are propagated through the film and mediated by the narrow interfaces between the different polymer layers.

We take advantage of the fact that the morphologies of diblock copolymers in ultrathin films have been extensively studied.[50,53−67] With symmetric diblock copolymers of poly(styrene-*block*-methyl methacrylate) (P(S-*b*-MMA)) and poly(styrene-*block*-2-vinylpyridine) (P(S-*b*-2VP)), it is well-known that a PS domain readily segregates to the free surface while a PMMA or P2VP domain segregates to the silica substrate interface.[56,61] Favorable interfacial interactions are maximized to the extent that a film forms holes and islands within the top layer[54,58] to accommodate the quantized film thickness of $L/2$, $3L/2$, $5L/2$, etc., where L is the lamellar period which scales with molecular weight[59] (M) as $L \sim M^{2/3}$. In comparison, the time scale for the self-assembly process has been the subject of only a few investigations.[60−62] Instead, studies more commonly measure "aggressively annealed" samples that have been heated far above T_g (e.g., 443 K) in excess of 24 h to ensure that the equilibrium morphology is acquired.[50,56,58]

In this investigation, we demonstrate that intrinsic excimer and monomer fluorescence from phenyl rings in the styrene blocks is useful in monitoring in situ the self-assembly of the lamellar morphology of thin styrene-containing block copolymers, e.g., P(S-*b*-MMA) and P(S-*b*-2VP), supported on silica. We also employ extrinsic probe or label fluorescence to compare T_g values within styrene domains of the resulting well-ordered, ultrathin diblock copolymer films with T_g values of PS layers with PS/PMMA and PS/P2VP multilayer films of equivalent morphology. We find that the T_gs of individual styrene block layers differ greatly in nanoconfined P(S-*b*-MMA) and P(S-*b*-2VP) films, indicating the importance of the polymer in the other blocks in dictating the T_g response in the styrene block domains. However, for a given system, e.g., PS/PMMA compared with P(S-*b*-MMA) or PS/P2VP compared with P(S-*b*-2VP), with identical layer thicknesses in the self-assembled block copolymer and multilayer film made from homopolymers, we find that the T_gs of individual PS layers are the same within error. This indicates that there is no additional effect of chain connectivity in the block copolymer relative to the homopolymer in modifying the T_g behavior of confined PS layers. Comparison of the T_g−nanoconfinement behavior of block copolymers with that of multilayer films of PS with PMMA or P2VP demonstrates that the enhanced mobility at an ultrathin PS (or styrene block domain) free-surface layer is present only when the PMMA or P2VP underlayer is sufficiently thin (∼10 nm thick) and the very strong P2VP−substrate interactions have been eliminated.

Experimental Section

Solutions of diblock copolymers of P(S-*b*-MMA) (Polymer Laboratories, reported peak $M = 113\,000$ g/mol, $M_w/M_n = 1.1$, 50 mol % styrene) dissolved in toluene and P(S-*b*-2VP) (Polymer Source, reported $M_n = 114\,000$ g/mol, $M_w/M_n = 1.08$, 50 mol % styrene) dissolved in 1,1,2-trichloroethane were spin-coated onto silica substrates. For T_g measurements, pyrene dye (<0.2% of dry polymer weight) was codissolved in solutions with block copolymers. The expected lamellar periods (L), based on measurements reported in the literature and scaled using $L \sim M_n^{2/3}$, are 40 nm[60] for P(S-*b*-MMA) and 56 nm[64,65] for P(S-*b*-2VP). The interfacial widths are taken to be 5.0 nm[50] for P(S-*b*-MMA) and 3.4 nm[49] for P(S-*b*-2VP).[68] Differential scanning calorimetry (DSC) measurements (Mettler-Toledo DSC822, second heat, onset method, 10 K/min) of the P(S-*b*-MMA) block copolymer revealed two T_g values at 375 and 391 K, which we attribute to the PS and PMMA domains, respectively. The P(S-*b*-2VP) block copolymer displayed one T_g by DSC at 372 K, consistent with the known T_g values of both PS and P2VP.

Multilayer films of homopolymer were assembled from P2VP (Scientific Polymer Products, reported $M_v = 200\,000$ g/mol, T_g by DSC = 374 K),[69] PMMA (Pressure Chemical, reported $M_w = 255\,000$ g/mol, $M_w/M_n \leq 1.15$, T_g by DSC = 393 K), and PS (neat or pyrene-labeled, synthesized by free-radical polymerization, T_g by DSC = 376 K).[70] The neat PS synthesized had $M_n = 265\,000$ g/mol and $M_w/M_n = 1.52$, as determined by gel permeation chromatography (GPC) (Waters) relative to PS standards. The copolymerization of styrene with 1-pyrenylbutyl methacrylate yielded polymer with 1 in 485 units being a pyrene-labeled methacrylate (determined by UV−vis spectroscopy), with $M_n = 247\,000$ g/mol and $M_w/M_n = 1.90$ (details of the synthesis are given in ref 15). The T_g measured by fluorescence of thick (>1000 nm) single-layer pyrene-labeled PS films was 374 K. Multilayer films of PS/PMMA homopolymers were made by spin-coating layers onto mica and floating them onto the underlying films via a water transfer process.[22] The PS/P2VP bilayer films were made by spin-coating a PS layer from toluene solution directly onto the underlying P2VP (toluene is a nonsolvent for P2VP). The films were annealed for 20 min at 418 K prior to the T_g measurements.

Steady-state fluorescence from the copolymer films, involving intrinsic fluorescence from the phenyl rings of the PS block domains or extrinsic fluorescence from pyrene dopant, was measured using a Photon Technology International fluorimeter at a nominal angle of incidence of 28°.[71] The measurements of multilayer homopolymer films containing pyrene-labeled PS employed a SPEX Fluorolog II fluorimeter in a front-face geometry. For intrinsic fluorescence, the phenyl rings were excited at 260 nm with emission collected from 270 to 390 nm using 1.5 mm slits (6 and 3 nm band-pass for excitation and emission, respectively) for the 500 nm thick films and 2 mm slits (8 and 4 nm band-pass for excitation and emission, respectively) for the 200 nm thick films. The pyrene dye (freely doped or labeled) was excited at 324 nm with emission collected from 360 to 460 nm using 2.5 mm slits (10 and 5 nm band-pass for excitation and emission, respectively) for film thicknesses less than 200 nm and 1.25 mm slits (5 and 2.5 nm band-pass for excitation and emission, respectively) for thicker films. The ultrathin layers of pyrene-labeled PS measured on the SPEX used 5 mm slits (9 nm band-pass).

The silica substrates were cleaned with base (10 wt % sodium hydroxide, 20 wt % water, 70 wt % ethyl alcohol) and acid (1 M HCl) solutions and rinsed thoroughly and then subsequently solvent-cleaned between experiments. Sample temperature in the fluorimeters was controlled to within ±0.2 K using a microprocessor-controlled (Minco products) Kapton ribbon heater with a resistance temperature controller. Film thicknesses were measured using a Tencor P10 profilometer or a Woollam M-2000D spectroscopic ellipsometer.

Results and Discussion

To investigate the T_gs within the PS block domains of self-assembled, multilayer block copolymers, we have used a free

pyrene dye that segregates into the PS domains upon self-assembly of the lamellar morphology. Block copolymer films made by spin-coating are initially disordered, and self-assembly of the lamellar morphology occurs when the films are heated far above T_g for an extended period of time. Some studies have employed an "aggressive annealing" procedure in which the samples are held at 443 K for times in excess of 24 h[50,56,58] in order to guarantee that the final morphology is obtained. However, use of a free pyrene dye limits the annealing time that the samples can be held at temperatures far above T_g. At 443 K, the polymer and dye are sufficiently mobile to allow for slow sublimation of the dye; aggressive annealing for many hours at 443 K does not leave any dye within the film for the subsequent measurements of T_g. We have found that intrinsic fluorescence from the phenyl rings of the PS blocks can be used to monitor in situ the self-assembly process. This allows us to determine optimum annealing conditions for our films in order to obtain the desired lamellar morphology with sufficient pyrene dye still present within the PS domains for the T_g measurements.

Time Scale for Self-Assembly Process: Intrinsic Fluorescence from Phenyl Ring of PS. The phenyl rings of PS absorb and fluoresce ultraviolet light, with the emission spectrum consisting of both monomer and excimer fluorescence. Monomer fluorescence is due to emission from a single excited phenyl ring, while excimer fluorescence is due to emission from an excited-state dimer formed when two phenyl rings are oriented in a parallel, sandwich-like conformation with an inter-ring separation distance of 3−4 Å, a condition that commonly occurs in PS-containing systems.[72,73] Consequently, intrinsic fluorescence has been used to monitor local chain conformations in dilute PS solutions.[73] Intrinsic fluorescence from phenyl rings has also recently been used to measure T_g values in ultrathin films of PS and styrene-containing random copolymers and to monitor in situ the stress relaxation during annealing of freshly spin-coated thin and ultrathin PS films.[30,74,75] Intrinsic phenyl ring fluorescence has also been shown to be useful in monitoring in situ the phase separation of immiscible blends containing PS, with an increase in the ratio of excimer to monomer fluorescence intensity, $I_{excimer}/I_{monomer}$, occurring with increasing phase separation, i.e., increasing local concentration of phenyl rings in PS-rich domains.[76,77] In a similar vein, we expect that the value of $I_{excimer}/I_{monomer}$ will increase during the self-assembly of thin or ultrathin films of styrene-containing diblock copolymers. Here we provide the first demonstration that intrinsic fluorescence can be used for such in situ monitoring.

Figure 1 shows the intrinsic fluorescence spectrum as a function of annealing time at 443 K of a 200 nm thick P(S-*b*-MMA) film supported on quartz. The block copolymer film is initially in a disordered state after spin-coating and is able to microphase separate upon heating to 443 K where the chains become sufficiently mobile. The spectra show an increase in excimer fluorescence intensity and a corresponding decrease in monomer fluorescence intensity with increasing annealing time, with little change in the spectra after ~30 min. Similar data were obtained for 500 nm thick P(S-*b*-MMA) films and 200 and 500 nm thick P(S-*b*-2VP) films.

We quantify the time scale for self-assembly by plotting $I_{excimer}/I_{monomer}$ as a function of time. The excimer intensity is taken as the intensity at 330 nm while the monomer intensity is taken as the intensity at 280 nm. Figure 2 shows data for 200 and 500 nm thick films of P(S-*b*-MMA) and P(S-*b*-2VP). Each data set has been fit to a single-exponential decay in order to extract a characteristic time τ for the self-assembly process.

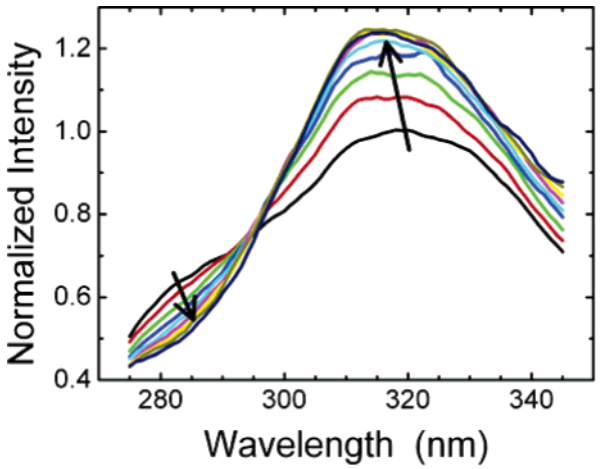

Figure 1. Intrinsic fluorescence emission spectra from phenyl rings on styrene repeat units in a 200 nm thick P(S-*b*-MMA) film as a function of annealing time at 443 K. The spin-coated film, in an initially disordered state, was heated to 443 K, and emission spectra were taken every 5 min, showing a decrease in monomer fluorescence (at ~280 nm) and an increase in excimer fluorescence (at ~320 nm) as the self-assembly process proceeds. (Spectra are normalized to the initial intensity at 320 nm.)

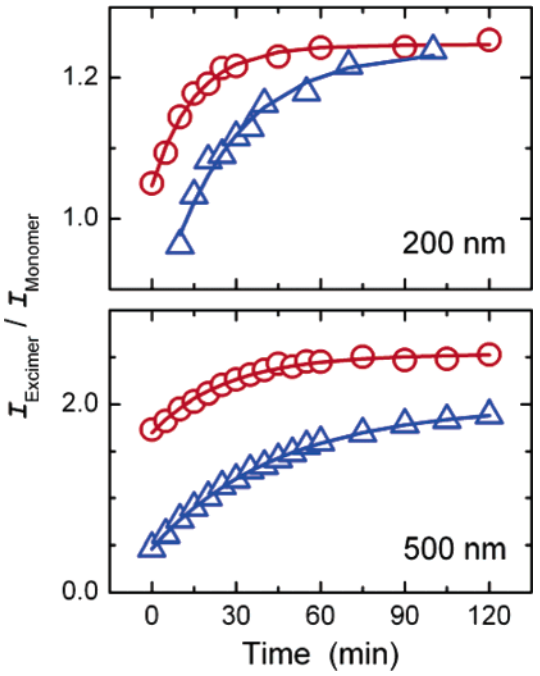

Figure 2. Ratio of excimer fluorescence intensity to monomer fluorescence intensity as a function of time for block copolymer films annealed at 443 K. Data are for 200 nm thick and 500 nm thick films of P(S-*b*-MMA) (circles) and P(S-*b*-2VP) (triangles). The 200 nm thick P(S-*b*-MMA) data correspond to the spectra shown in Figure 1. The curves represent the fit of each data set to a single-exponential function which was used to extract a characteristic time scale for the self-assembly process.

Using intrinsic fluorescence, the characteristic self-assembly time scale τ for 200 nm thick P(S-*b*-MMA) films was measured to be 15 ± 1 min.[78] A time of $2\tau = 30$ min, corresponding to ~90% of the total change in $I_{excimer}/I_{monomer}$ during self-assembly, agrees well with the limited data available on the time scale for self-assembly of similar systems. Using neutron reflectivity, Mayes et al.[60] measured the neutron reflectivity profile of partially annealed films of symmetric P(S-*b*-MMA) of similar molecular weight. The scattering profiles for a 68 nm thick film at 0, 0.1, 0.25, 0.5, 1, and 16 h indicate that the morphology is

essentially formed after ~30 min at 443 K. (We cannot make a direct comparison with the result of Mayes et al.[60] by employing 68 nm thick films in our own studies because the fluorescence intensity at 443 K is insufficient to obtain a low noise to signal ratio in such ultrathin films.)

At a thickness of 200 nm, the P(S-*b*-2VP) films were found to require almost twice as long to self-assemble at 443 K than the P(S-*b*-MMA) films: $\tau = 26 \pm 4$ min for 200 nm thick P(S-*b*-2VP) films while $\tau = 15 \pm 1$ min for 200 nm thick P(S-*b*-MMA) films. No related study of the self-assembly of P(S-*b*-2VP) films has been reported in the literature. However, our observation is in agreement with cross-sectional transmission electron microscopy (TEM) measurements[61] of 154 nm thick P(S-*b*-4VP) films supported on mica in which it was observed that the PS domain assembled at the air interface faster than the P4VP domain assembled at the mica interface. In ref 61, the sluggish ordering of the P4VP domain at the interface was attributed to the strong attractive interactions with the mica substrate hindering the dynamics. This is a reasonable assumption because the T_gs of ultrathin P2VP films on substrates with hydroxyl groups present on the substrate surfaces increase with decreasing film thickness.[17−19] However, it should be noted that the T_g of bulk P4VP is significantly higher (411 K[61]) than that of P2VP or PS (both ~373 K). The TEM measurements of 154 nm thick P(S-*b*-4VP) films indicated that the final morphology was reached after 40 min at 443 K.[61]

We found that 500 nm thick diblock copolymer films required significantly longer time scales to self-assemble than 200 nm thick diblock copolymer films. In the case of P(S-*b*-MMA), $\tau = 27 \pm 2$ min for 500 nm thick films vs $\tau = 15 \pm 1$ min for 200 nm thick films. In the case of P(S-*b*-2VP), $\tau = 50 \pm 8$ min for 500 nm thick films vs $\tau = 26 \pm 4$ min for 200 nm thick films. These results are intuitively appealing because it has been demonstrated that the self-assembly process starts at the free surface and substrate interface and progresses inward.[57,61]

On the basis of the intrinsic fluorescence measurements of the time scale for the self-assembly process, we have chosen to anneal the P(S-*b*-MMA) films for 30 min and the P(S-*b*-2VP) films for 60 min at 443 K prior to performing T_g measurements. For 200 nm thick films, this length of time corresponds to approximately $2\tau \approx 90\%$ of the overall change in $I_{excimer}/I_{monomer}$ during self-assembly. As thinner films self-assemble more readily, we believe that nanoscale films (with thickness <100 nm) will be fully or nearly fully self-assembled prior to the T_g measurement. We note that use of longer annealing times at 443 K for films thicker than 200 nm did not result in any change in the measured T_g values.

Segregation of Pyrene Dye to PS Domains and Measurement of T_g. Pyrene dye was incorporated as dopant into the block copolymer films at trace levels (<0.2% of dry polymer weight) in order to perform T_g measurements. This was accomplished by codissolving a small amount of pyrene dye into the block copolymer solution prior to spin-coating. It was found that the pyrene dye segregated into the PS domains upon heating the films to 443 K in order to self-assemble the morphology. This was confirmed by comparing the relative peak intensities of the pyrene spectra incorporated into films of different polymers.

It is well-known that the relative peak intensities of the pyrene fluorescence emission spectrum are sensitive to the local polarity of the environment surrounding the dye.[74,79] Specifically, the intensity of the 0−0 band (first peak, ~375 nm) is enhanced at the expense of other peaks when pyrene is in a more polar environment, such as PMMA or P2VP. Figure 3 shows the room temperature fluorescence spectrum from 370 to 390 nm of pyrene doped into 500 nm thick films of PMMA, P2VP, and PS as well as P(S-*b*-MMA) and P(S-*b*-2VP) after self-assembly of the lamellar morphology. The fluorescence intensity of each spectrum has been normalized to unity at the third peak (~385 nm), which has been shown to be independent of local polarity.[79] The ratios of intensities of the first peak (~375 nm) relative to the third peak (~385 nm) are 1.34 in PMMA, 1.36 in P2VP, 1.02 in PS, and 1.12 in both P(S-*b*-MMA) and P(S-*b*-2VP). These values indicate that the pyrene dye is predominantly located within the PS domains of the diblock copolymer films. Segregation of pyrene into the PS domains of P(S-*b*-2VP) films was also reported by Nakashima et al.[63]

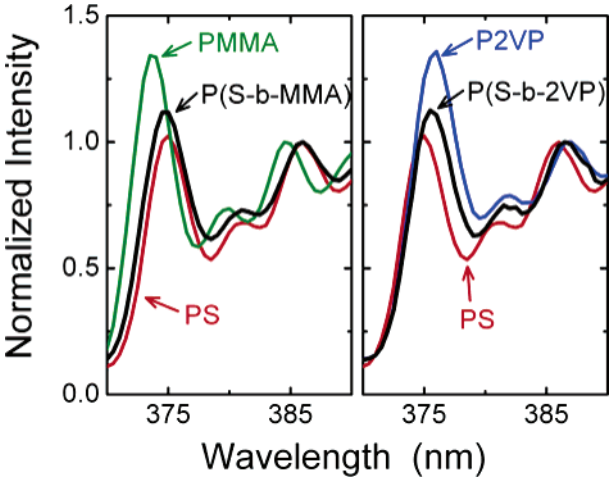

Figure 3. Fluorescence emission spectra of pyrene dye taken at room temperature in 500 nm thick films of PMMA (green curve), P2VP (blue curve), PS (red curves), and both block copolymers, P(S-*b*-MMA) and P(S-*b*-2VP), after self-assembling into lamellar morphology (black curves). Spectra demonstrate that the pyrene dye segregates into the PS domains upon self-assembly, since the peak intensity of the first peak at ~375 nm relative to the third peak at ~385 nm is sensitive to the local polarity of the surrounding environment.[79] (Spectra were normalized to the third peak at ~385 nm.)

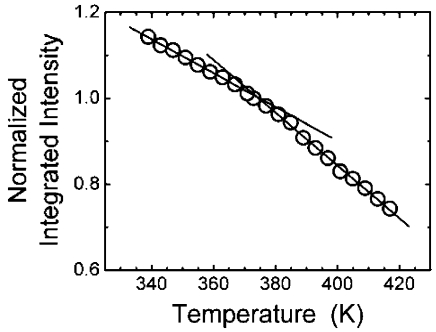

Figure 4. Normalized integrated fluorescence intensity of a trace level of pyrene dye as a function of temperature measured upon cooling for a 355 nm thick P(S-*b*-MMA) film. The data indicate that $T_g = 374 \pm 2$ K for the PS domains (integrated intensity normalized to unity at 373 K).

The T_g measurements via fluorescence of the pyrene dye were performed on P(S-*b*-MMA) and P(S-*b*-2VP) films by annealing the films at 443 K to self-assemble the morphology (as outlined above) and then cooling the films to 418 K and obtaining pyrene spectra every 5 K on cooling. The T_g is identified by the intersection of the linear increases in integrated fluorescence intensity with decreasing temperature in the rubbery and glassy states, as described in refs 15, 16, and 40−44. Figure 4 shows a typical plot of integrated fluorescence intensity as a function of temperature for a 355 nm thick P(S-*b*-MMA) film, indicating

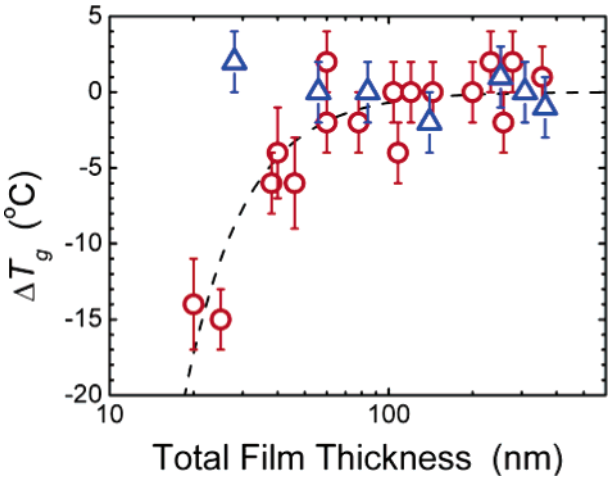

Figure 5. $\Delta T_g = T_g - T_g^{bulk}$ for PS domains as a function of total block copolymer film thickness in P(S-*b*-2VP) films (triangles) and P(S-*b*-MMA) films (circles). The dashed curve represents data for PS homopolymer films from refs 15 and 16.

that the T_g of the PS domains is 374 ± 2 K. (At the end of the measurement done upon cooling, the temperature is returned to 418 K to confirm that the fluorescence intensity is recovered, and within error no pyrene dye sublimed over the temperature range used to determine T_g.)

The $\Delta T_g = T_g - T_g^{bulk}$ values of the PS domains in both P(S-*b*-MMA) and P(S-*b*-2VP) films are plotted in Figure 5 as a function of total block copolymer film thickness. The value of T_g^{bulk} is taken as the average of the T_g values measured for the PS domains with total block copolymer film thickness greater than 200 nm: 373 K for P(S-*b*-MMA) and 370 K for P(S-*b*-2VP). We find that the PS domains located within the P(S-*b*-2VP) films exhibit no change, within experimental uncertainty, with decreasing film thickness while the PS domains located within the P(S-*b*-MMA) films show a substantial decrease in T_g with decreasing film thickness.[80] The dashed curve represents data from refs 15 and 16 for single-layer PS homopolymer films measured using fluorescence of pyrene:

$$\Delta T_g = -373\ \text{K}\ (4.3/h)^{2.0} \qquad (1)$$

The data in Figure 5 demonstrate the important effect of the type of polymer attached to the PS block on the T_g−nanoconfinement behavior in P(S-*b*-MMA) and P(S-*b*-2VP) films. In comparison with PS homopolymer films, the presence of the PMMA block has little or no impact, with the T_g of the PS domains within P(S-*b*-MMA) films exhibiting the same behavior as PS homopolymer in single-layer films of the same total film thickness. In contrast, the presence of the P2VP block completely suppresses the T_g reduction typically exhibited by PS, eliminating the enhanced mobility present at the free surface of PS. This is especially noteworthy in the case of the 28 nm thick P(S-*b*-2VP) film, in which the PS units are confined to the free-surface layer or to the interfacial region between the surface layer containing PS blocks and the substrate layer containing P2VP blocks; i.e., none of the styrene units are located underneath a P2VP domain.

The thinnest block copolymer films with complete layers are *L*/2 in thickness, which corresponds to a 20 nm thick film for P(S-*b*-MMA) and a 28 nm thick film for P(S-*b*-2VP). The morphologies of these thinnest block copolymer films are equivalent to bilayer films of PS/PMMA and PS/P2VP, as illustrated in Figure 6a,b. The next thinnest complete layer morphology for the block copolymer films is 3*L*/2, corresponding to a 60 nm thick film for P(S-*b*-MMA) and an 84 nm thick film for P(S-*b*-2VP). The films corresponding to 3*L*/2 in thickness exhibit essentially bulk T_g of the PS domains. The P(S-*b*-MMA) films of intermediate thickness (~40 nm) consist of regions[54,58] that are 20 nm (*L*/2) and 60 nm (3*L*/2) in thickness with the overall T_g values corresponding to a linear combination of these two results. To within experimental error, we are only able resolve a single, broad T_g for these P(S-*b*-MMA) films of intermediate thickness because the difference in T_g values between the 20 and 60 nm thick films is <15 K. Thus, in order to understand the results of Figure 5, it suffices to explain the difference between the two bilayer film results corresponding to *L*/2 in block copolymer film thickness.

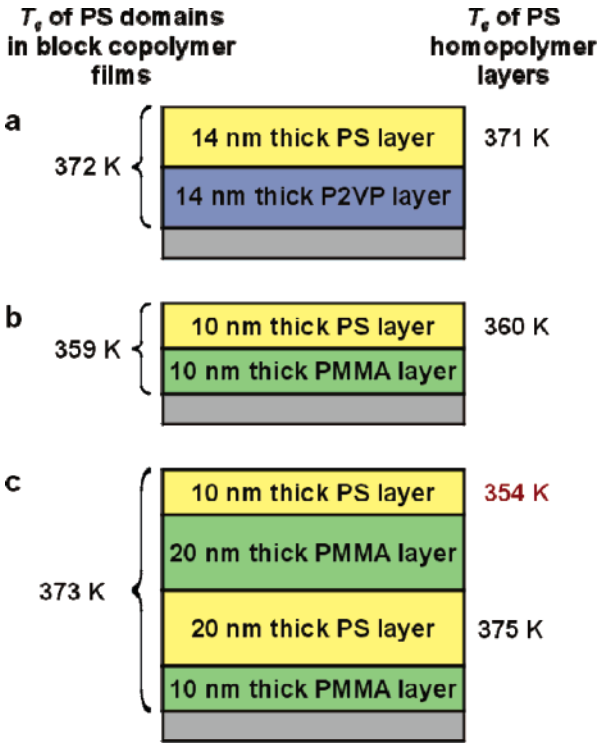

Figure 6. Schematic of lamellar morphology for three of the thinnest block copolymer films measured: 28 nm thick (*L*/2) P(S-*b*-2VP), and 20 nm (*L*/2) and 60 nm (3*L*/2) thick P(S-*b*-MMA) films. The T_gs measured using fluorescence of free pyrene dye segregated to PS blocks of block copolymer films are indicated on the left of the figure. Identical multilayer morphologies were assembled by hand from homopolymer films using a pyrene-labeled PS to measure the T_g of the individual PS layers. The T_g values for PS homopolymer layers are given on the right of the figure.

Comparison of Block Copolymer Films to Multilayer Films of Different Homopolymers with Equivalent Morphology. In order to understand better the observed T_g behavior of the PS domains within the block copolymer films, we have made multilayer films assembled from homopolymers which have equivalent morphologies. By employing a PS homopolymer that has been labeled at trace levels with a pyrenyl dye, we are able to measure the T_g values of select PS layers within these multilayer films. Figure 6 illustrates the morphologies of these multilayer films. The morphologies of the thinnest block copolymer films (*L*/2 in thickness) were simulated by making bilayer films of a 10 nm thick pyrene-labeled PS layer sitting atop a 10 nm thick PMMA layer and a 14 nm thick pyrene-labeled PS layer sitting atop a 14 nm thick P2VP layer. The T_gs of the pyrene-labeled PS surface layers were 360 ± 2 K for the PS/PMMA bilayer film and 371 ± 2 K for the PS/P2VP bilayer film. Both values are in excellent agreement with our T_g measurements of the PS domains within the block copolymer

films: 359 ± 3 K for P(S-*b*-MMA) and 372 ± 2 K for P(S-*b*-2VP).

The next thinnest complete layer morphology for the P(S-*b*-MMA) block copolymer films is 3*L*/2 (60 nm total thickness). This multilayer morphology is considerably more complicated with two PS layers and two PMMA layers, as illustrated in Figure 6c. We have made two types of 60 nm thick PS/PMMA/PS/PMMA homopolymer multilayer films with this morphology. In one we have placed the pyrene-labeled PS in the 10 nm thick PS surface layer and used neat PS for the 20 nm thick interlayer, and in the other we have placed the pyrene-labeled PS in the 20 nm thick interlayer and used neat PS for the 10 nm thick PS surface layer. This has allowed us to probe selectively the T_gs of the two PS layers independently. We find that the T_g of the 20 nm thick interior layer is 375 ± 2 K, which is in excellent agreement with the T_g observed for 60 nm thick P(S-*b*-MMA) block copolymer films, 373 ± 2 K. However, the 10 nm thick PS surface layer exhibits a significantly lower $T_g = 354 \pm 2$ K. Measurements of 60 nm thick P(S-*b*-MMA) block copolymer films did not reveal a second transition at this lower temperature. This discrepancy is likely because we cannot isolate the fluorescence signal from only the top 10 nm thick PS surface domain in the block copolymer films, since most of the fluorescence signal will be originating from the 20 nm thick PS middle domain.[81] In addition, the contrast of the glass transition for the top 10 nm thick PS surface domain is expected to be extremely weak.[15] Unfortunately, with the difficulties associated with floating P2VP off mica substrates, we are unable to make PS/P2VP multilayer geometries containing more than one P2VP layer.

The T_g values measured for the PS domains within the block copolymer films and the PS layers within the multilayer films of different homopolymers appear to be the same within experimental uncertainty. This indicates that there is no effect of chain connectivity across the interface (present in block copolymers but absent in multilayer homopolymer films) on the cooperative segmental dynamics within individual layers/domains. In addition, the slightly extended chain conformations of the block copolymers within the lamellar morphology[53] have no impact on T_g. This equivalence between the measured T_g values of the PS domains within the block copolymer films and the PS layers of the multilayer films of different homopolymers allows us to use homopolymer multilayer films to investigate the difference in the T_g−nanoconfinement behavior between the P(S-*b*-MMA) and P(S-*b*-2VP) block copolymer films. The results of the thinnest films in Figure 5 indicate that the 14 nm thick P2VP underlayer significantly modifies the T_g−nanoconfinement behavior of the PS surface layer, eliminating the enhanced mobility observed at the free surface of PS films relative to bulk PS.[15] In contrast, the 10 nm thick PMMA underlayer has little impact in modifying the T_g reduction of the PS surface layer compared with that of single-layer PS films.

On the basis of how free-surface effects and substrate interactions impact the T_g of ultrathin single-layer homopolymer films of PS,[13] PMMA,[14] and P2VP,[17,19] the simplest explanation for the results presented in Figure 5 is that the strong P2VP−silica substrate interaction prevents the T_g reduction typically present at the free surface of PS and that the significantly weaker PMMA−silica substrate interaction is unable to do the same. However, this explanation is incomplete. We have performed measurements of PS/P2VP and PS/PMMA bilayer films[19] which indicate that both P2VP and PMMA underlayers modify the T_g of a PS surface layer to the same extent when they are sufficiently thick. In the PS/P2VP and PS/PMMA bilayer film studies, we found that 14 nm thick surface layers of PS supported on 500 nm thick P2VP or 500 nm thick PMMA underlayers show a near elimination of the large (~32 K) T_g reduction observed for 14 nm thick PS surface layers supported on bulk PS.[19] This finding indicates that the T_g reduction of the PS free-surface layer can be suppressed by the different underlying material when it is sufficiently thick to exhibit bulk behavior. Thus, strong interactions present at the substrate interface are not necessary to account for a bulk T_g response of a PS free-surface layer. This statement is also valid when the underlayer films are 46 nm thick instead of 500 nm thick.[19] The results of ref 19 demonstrate that the T_g response of the PS free-surface layer is dependent on what *type* of material (PS vs PMMA or P2VP) is present in the underlayer.

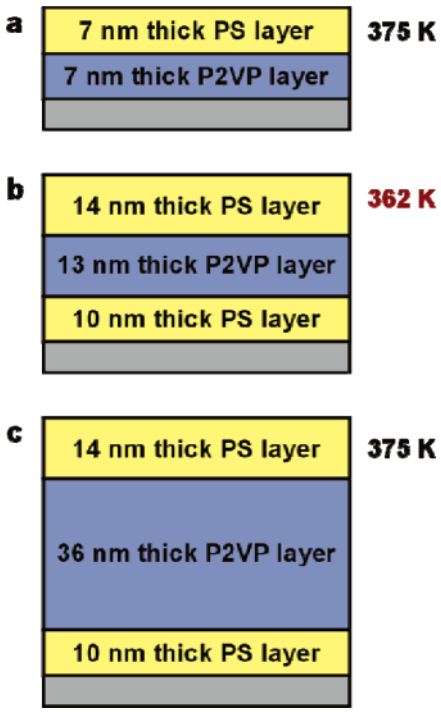

Figure 7. T_g values of pyrene-labeled PS free-surface layers for PS/P2VP bilayer and PS/P2VP/PS trilayer films of homopolymers, demonstrating that when the P2VP−silica substrate interaction is removed, the PS free-surface layer can support a substantial T_g reduction only when the P2VP underlayer is sufficiently thin.

The results presented in Figures 5 and 6 for the P(S-*b*-MMA) block copolymer and the PS/PMMA bilayer films indicate that the *amount* of material underneath the PS free-surface layer is also important. When the PMMA underlayer is reduced to ~10 nm, it is no longer sufficiently thick to prevent the PS free-surface layer from exhibiting a strong T_g reduction. Changes in the T_g−nanoconfinement behavior upon confinement to layer thicknesses comparable to ~10 nm have been observed previously with PS/PS bilayer films in ref 15, which demonstrated that when the overall film thickness becomes sufficiently small (a few tens of nanometers or less), the film is no longer able to support a substantial gradient in the cooperative segmental dynamics and the T_gs across the film become more homogeneous. We have tested the effect of extreme confinement of PS/P2VP bilayer films by measuring the T_g of a 7 nm thick PS free-surface layer atop a 7 nm thick P2VP underlayer (Figure 7a), but even at this extreme confinement the T_g of the PS free-surface layer is essentially bulk: $T_g = 375 \pm 2$ K.[82] However, if the strong P2VP−silica substrate interaction is removed by placing a 10 nm thick PS layer at the substrate,[83] we find that the PS free-surface layer of a PS/P2VP/PS trilayer film exhibits

a reduced T_g when the P2VP underlayer film is made sufficiently thin. Figure 7b demonstrates that a 14 nm thick PS free-surface layer exhibits $T_g = 362 \pm 2$ K, well below T_g^{bulk}, when supported on a 13 nm thick layer of P2VP atop a 10 nm thick layer of PS. In contrast, when the P2VP middle layer is made thicker (e.g., 36 nm thick as in Figure 7c), the T_g reduction relative to T_g^{bulk} of the 14 nm thick PS free-surface layer is eliminated: $T_g = 375 \pm 2$ K. This is consistent with the results of ref 19, which showed no T_g reduction for 14 nm thick ultrathin PS free-surface layers when supported on bulk (500 nm thick) P2VP underlayers. Figure 7 demonstrates that when the P2VP−silica substrate interaction is removed, the PS free-surface layer can support a substantial T_g reduction only when the P2VP underlayer film is sufficiently thin. We note that the trilayer geometry with PS at the silica substrate interface as shown in Figure 7c would never be obtained using self-assembled block copolymers because a P2VP block would always segregate to the substrate interface in order to maximize favorable interactions.

The results of Figures 5−7 collectively indicate that when the underlayer thickness is sufficiently small (∼10 nm), these ultrathin underlayers of PMMA and P2VP are unable to prevent a PS free surface from exhibiting a T_g reduction. However, if a strong substrate interaction such as that at the P2VP−silica interface is present, it dominates the behavior when the underlayer is ultrathin and prevents any T_g reduction at the PS free surface from occurring. Thus, both the *type* and *amount* of material present in the underlayer determine the T_g−confinement behavior at the free surface of multilayer films. Other recent studies of multilayer films have also shown large changes in properties with decreasing layer thickness. Hiltner and co-workers[3,4] have observed increased gas permeation and merging of the dynamics into a single T_g when the thickness of the nanolayers is reduced, and Adhikari et al.[5] have observed craze propagation across multiple layers when the layer thickness is decreased. Why do the cooperative segmental dynamics behave fundamentally different when the layer/domain thicknesses reach <∼10 nm? We suggest that this critical thickness may be related to the size of the interfacial width between the two polymers. Under such circumstances, multilayer films or nanostructured blends with a significant fraction of interface ("interphase") may have properties that are more typical of single-component materials with intermediate properties than those of their more heterogeneous counterparts with larger domain sizes or layer thicknesses that can exhibit distinct properties associated with each domain or layer. Studies to address this hypothesis are underway.

These results demonstrate that the T_g reduction in a free surface layer of PS can be tuned significantly by changing the thickness and identity of the underlying polymer support. Thus, it is evident that the enhanced cooperative segmental mobility within a free surface layer is more complex than the simple assertion that a reduced T_g is always present within a few nanometers of a polymer−air interface. This study shows that the length scale of the T_g−confinement phenomenon is impacted by the presence of material that is at least several tens of nanometers away.

Summary

We have shown that intrinsic fluorescence from styrene blocks is a simple, effective method to quantify in situ the time scale for self-assembly of styrene-containing block copolymers. Measurements of the self-assembly process in thin films of symmetric diblock copolymer reveal that P(S-*b*-2VP) films require nearly twice as long to assemble than P(S-*b*-MMA) films of equal thickness. This is likely due to the stronger favorable interactions of the P2VP domain with the silica substrate hindering the dynamics at the substrate interface. The self-assembly of thicker films (500 vs 200 nm thick films) is also slower, consistent with the self-assembly process starting at the surface and substrate interfaces and propagating inward.

A free pyrene dye, which segregates into PS domains upon self-assembly, was employed to measure the T_g of the PS lamellar domains within P(S-*b*-MMA) and P(S-*b*-2VP) films. The T_g of the PS domains within the P(S-*b*-MMA) films was found to decrease with decreasing film thickness following the same T_g reductions observed for single-layer PS homopolymer films; in contrast, the T_g of the PS domains within the P(S-*b*-2VP) films showed no T_g reduction upon nanoscale confinement. The block copolymer films were compared to multilayer films of equivalent morphology fabricated from homopolymer layers. Excellent agreement was obtained between the T_gs measured for the PS layers within the multilayer films made from different homopolymers and the PS domains within the block copolymer films. This indicates that there is no effect of chain connectivity between blocks in the copolymers on the cooperative segmental dynamics across the narrow immiscible interface. Comparisons with bilayer and trilayer films of varying thickness demonstrate that both the *type* and *amount* of material present in the underlayers determine the T_g−nanoconfinement behavior at the free surface of multilayer films. When underlayers of PMMA supported on silica are reduced to thicknesses of ∼10 nm, they lose the ability to suppress the enhanced mobility of a PS free-surface layer, which is also true for P2VP underlayers when the strong P2VP−silica substrate interaction is removed. These observations have important implications for the design of multilayer films and nanostructured blends and indicate a means by which the T_g reduction at a PS free surface may be tuned.

Acknowledgment. We acknowledge the support of Northwestern University and the NSF-MRSEC program (Grant DMR-050513). We also thank Robert Sandoval for helping with the synthesis of the pyrene-labeled PS.

References and Notes

(1) Harrats, C.; Thomas, S.; Groeninckx, G. *Micro- and Nanostructured Multiphase Polymer Blend Systems: Phase Morphology and Interfaces*; Taylor & Francis: New York, 2006.
(2) Weber, M. F.; Stover, C. A.; Gilbert, L. R.; Nevitt, T. J.; Ouderkirk, A. J. *Science* **2000**, *287*, 2451−2456.
(3) Liu, R. Y. F.; Jin, Y.; Hiltner, A.; Baer, E. *Macromol. Rapid Commun.* **2003**, *24*, 943−948.
(4) Liu, R. Y. F.; Bernal-Lara, T. E.; Hiltner, A.; Baer, E. *Macromolecules* **2004**, *37*, 6972−6979.
(5) Adhikari, R.; Henning, S.; Michler, G. H. *Macromol. Symp.* **2006**, *233*, 26−35.
(6) Tao, Y.; Kim, J.; Torkelson, J. M. *Polymer* **2006**, *47*, 6773−6781.
(7) Shimizu, H.; Li, Y. J.; Kaito, A.; Sano, H. *Macromolecules* **2005**, *38*, 7880−7883.
(8) Ruzette, A.-V.; Leibler, L. *Nat. Mater.* **2005**, *4*, 19−31.
(9) Leibler, L. *Prog. Polym. Sci.* **2005**, *30*, 898−914.
(10) Baschnagel, J.; Varnik, F. *J. Phys.: Condens. Matter* **2005**, *17*, R851−R953.
(11) Roth, C. B.; Dutcher, J. R. *J. Electroanal. Chem.* **2005**, *584*, 13−22.
(12) Alcoutlabi, M.; McKenna, G. B. *J. Phys.: Condens. Matter* **2005**, *17*, R461−R524.
(13) Keddie, J. L.; Jones, R. A. L.; Cory, R. A. *Europhys. Lett.* **1994**, *27*, 59−64.
(14) Keddie, J. L.; Jones, R. A. L.; Cory, R. A. *Faraday Discuss.* **1994**, *98*, 219−230.
(15) Ellison, C. J.; Torkelson, J. M. *Nat. Mater.* **2003**, *2*, 695−700.
(16) Ellison, C. J.; Mundra, M. K.; Torkelson, J. M. *Macromolecules* **2005**, *38*, 1767−1778.
(17) van Zanten, J. H.; Wallace, W. E.; Wu, W.-L. *Phys. Rev. E* **1996**, *53*, R2053−R2056.

(18) Park, C. H.; Kim, J. H.; Ree, M.; Sohn, B.-H.; Jung, J. C.; Zin, W.-C. *Polymer* **2004**, *45*, 4507−4513.
(19) Roth, C. B.; McNerny, K. L.; Jager, W. F.; Torkelson, J. M. *Macromolecules* **2007**, *40*, 2568−2574.
(20) Grohens, Y.; Hamon, L.; Reiter, G.; Soldera, A.; Holl, Y. *Eur. Phys. J. E* **2002**, *8*, 217−224.
(21) Fukao, K.; Miyamoto, Y. *Phys. Rev. E* **2000**, *61*, 1743−1754.
(22) Forrest, J. A.; Dalnoki-Veress, K.; Dutcher, J. R. *Phys. Rev. E* **1997**, *56*, 5705−5716.
(23) Dalnoki-Veress, K.; Forrest, J. A.; Murray, C.; Gigault, C.; Dutcher, J. R. *Phys. Rev. E* **2001**, *63*, 031801.
(24) Roth, C. B.; Dutcher, J. R. *Eur. Phys. J. E* **2003**, *12*, S103−S107.
(25) Roth, C. B.; Pound, A.; Kamp, S. W.; Murray, C. A.; Dutcher, J. R. *Eur. Phys. J. E* **2006**, *20*, 441−448.
(26) Fryer, D. S.; Peters, R. D.; Kim, E. J.; Tomaszewski, J. E.; de Pablo, J. J.; Nealey, P. F.; White, C. C.; Wu, W.-L. *Macromolecules* **2001**, *34*, 5627−5634.
(27) Tsui, O. K. C.; Russell, T. P.; Hawker, C. J. *Macromolecules* **2001**, *34*, 5535−5539.
(28) Tate, R. S.; Fryer, D. S.; Pasqualini, S.; Montague, M. F.; de Pablo, J. J.; Nealey, P. F. *J. Chem. Phys.* **2001**, *115*, 9982−9990.
(29) Ellison, C. J.; Ruszkowski, R. L.; Fredin, N. J.; Torkelson, J. M. *Phys. Rev. Lett.* **2004**, *92*, 095702.
(30) Mundra, M. K.; Ellison, C. J.; Behling, R. E.; Torkelson, J. M. *Polymer* **2006**, *47*, 7747−7759.
(31) Tanaka, K.; Tsuchimura, Y.; Akabori, K.-I.; Ito, F.; Nagamura, T. *Appl. Phys. Lett.* **2006**, *89*, 061916.
(32) Sasaki, T.; Kawagoe, S.; Mitsuya, H.; Irie, S.; Sakurai, K. *J. Polym. Sci., Part B: Polym. Phys.* **2006**, *44*, 2475−2485.
(33) Wang, L.-M.; He, F.; Richert, R. *Phys. Rev. Lett.* **2004**, *92*, 095701.
(34) Arndt, M.; Stannarius, R.; Groothues, H.; Hempel, E.; Kremer, F. *Phys. Rev. Lett.* **1997**, *79*, 2077−2080.
(35) Marceau, S.; Tortai, J.-H.; Tillier, J.; Vourdas, N.; Gogolides, E.; Raptis, I.; Beltsios, K.; van Werden, K. *Microelectron. Eng.* **2006**, *83*, 1073−1077.
(36) Blum, F. D.; Young, E. N.; Smith, G.; Sitton, O. C. *Langmuir* **2006**, *22*, 4741−4744.
(37) Ash, B. J.; Schadler, L. S.; Siegel, R. W. *Mater. Lett.* **2002**, *55*, 83−87.
(38) Campoy-Quiles, M.; Sims, M.; Etchegoin, P. G.; Bradley, D. D. C. *Macromolecules* **2006**, *39*, 7673−7680.
(39) Hall, D. B.; Hooker, J. C.; Torkelson, J. M. *Macromolecules* **1997**, *30*, 667−669.
(40) Ellison, C. J.; Torkelson, J. M. *J. Polym. Sci., Part B: Polym. Phys.* **2002**, *40*, 2745−2758.
(41) Mundra, M. K.; Donthu, S. K.; Dravid, V. P.; Torkelson, J. M. *Nano Lett.* **2007**, *7*, 713−718.
(42) Rittigstein, P.; Priestley, R. D.; Broadbelt, L. J.; Torkelson, J. M. *Nat. Mater.* **2007**, *6*, 278−282.
(43) Ellison, C. J.; Kim, S. D.; Hall, D. B.; Torkelson, J. M. *Eur. Phys. J. E* **2002**, *8*, 155−166.
(44) Rittigstein, P.; Torkelson, J. M. *J. Polym. Sci., Part B: Polym. Phys.* **2006**, *44*, 2935−2943.
(45) Priestley, R. D.; Broadbelt, L. J.; Torkelson, J. M. *Macromolecules* **2005**, *38*, 654−657.
(46) Priestley, R. D.; Ellison, C. J.; Broadbelt, L. J.; Torkelson, J. M. *Science* **2005**, *309*, 456−459.
(47) Huang, Y.; Paul, D. R. *Polymer* **2004**, *45*, 8377−8393.
(48) Kawana, S.; Jones, R. A. L. *Eur. Phys. J. E* **2003**, *10*, 223−230.
(49) Dai, K. H.; Norton, L. J.; Kramer, E. J. *Macromolecules* **1994**, *27*, 1949−1956.
(50) Anastasiadis, S. H.; Russell, T. P.; Satija, S. K.; Majkrzak, C. F. *J. Chem. Phys.* **1990**, *92*, 5677−5691.
(51) Zhang, J.; Lodge, T. P.; Macosko, C. W. *J. Rheol.* **2006**, *50*, 41−57.
(52) Decher, G. *Science* **1997**, *277*, 1232−1237.
(53) Bates, F. S.; Fredrickson, G. H. *Annu. Rev. Phys. Chem.* **1990**, *41*, 525−557.
(54) Green, P. F.; Limary, R. *Adv. Colloid Interface Sci.* **2001**, *94*, 53−81.
(55) Fasolka, M. J.; Mayes, A. M. *Annu. Rev. Mater. Res.* **2001**, *31*, 323−355.
(56) Anastasiadis, S. H.; Russell, T. P.; Satija, S. K.; Majkrzak, C. F. *Phys. Rev. Lett.* **1989**, *62*, 1852−1855.
(57) Menelle, A.; Russell, T. P.; Anastasiadis, S. H.; Satija, S. K.; Majkrzak, C. F. *Phys. Rev. Lett.* **1992**, *68*, 67−70.
(58) Coulon, G.; Collin, B.; Ausserré, D.; Chatenay, D.; Russell, T. P. *J. Phys. (Paris)* **1990**, *51*, 2801−2811.
(59) Mayes, A. M.; Russell, T. P.; Deline, V. R.; Satija, S. K.; Majkrzak, C. F. *Macromolecules* **1994**, *27*, 7447−7453.
(60) Mayes, A. M.; Russell, T. P.; Bassereau, P.; Baker, S. M.; Smith, G. S. *Macromolecules* **1994**, *27*, 749−755.
(61) Sohn, B.-H.; Seo, B.-W.; Yoo, S. I.; Zin, W.-C. *Langmuir* **2002**, *18*, 10505−10508.
(62) Müller-Buschbaum, P.; Gutmann, J. S.; Lorenz-Haas, C.; Mahltig, B.; Stamm, M.; Petry, W. *Macromolecules* **2001**, *34*, 7463−7470.
(63) Nakashima, K.; Winnik, M. A.; Dai, K. H.; Kramer, E. J.; Washiyama, J. *Macromolecules* **1992**, *25*, 6866−6870.
(64) de Jeu, W. H.; Lambooy, P.; Vaknin, D. *Macromolecules* **1993**, *26*, 4973−4974.
(65) Anastasiadis, S. H.; Retsos, H.; Toprakcioglu, C.; Menelle, A.; Hadziioannou, G. *Macromolecules* **1998**, *31*, 6600−6604.
(66) Tanaka, K.; Takahara, A.; Kajiyama, T. *Acta Polym.* **1995**, *46*, 476−482.
(67) Miwa, Y.; Yamamoto, K.; Sakaguchi, M.; Sakai, M.; Tanida, K.; Hara, S.; Okamoto, S.; Shimada, S. *Macromolecules* **2004**, *37*, 831−839.
(68) As reviewed by Stamm and Schubert [Stamm, M.; Schubert, D. W. *Annu. Rev. Mater. Sci.* **1995**, *25*, 325−356], the interfacial width of PS/PMMA systems has been studied by many groups and techniques, with the most reliable measurements by neutron reflectivity reporting a value of 5.0 ± 0.3 nm.[50] To within experimental error, the same value has been measured in both PS/PMMA homopolymer bilayer systems and P(S-*b*-MMA) diblock copolymers.[50] The few measurements reported for PS/P2VP systems are less consistent: 3.4 nm for PS/P2VP homopolymer bilayers,[49] 4.5 ± 0.3 nm for P(S-*b*-2VP) diblock copolymers,[65] and 2.8 ± 0.3 nm for P(2VP-S-2VP) triblock systems.[65] These differences have been attributed to thermal fluctuations at the interface.[65] Because PS/P2VP is known to be a more strongly segregating system than PS/PMMA,[49,50] we take 3.4 nm to be a reasonable estimate of the interfacial width in PS/P2VP systems.
(69) The received material was dried in a vacuum oven at ∼110 °C to remove residual monomer.
(70) The molecular weights of the homopolymers were chosen to be sufficiently high such that dewetting of the multilayer geometries would not occur during the course of the experiment (maximum time of 20 min at T_g + 40 K).
(71) For the intrinsic fluorescence measurements, the angle of incidence was varied slightly from 28°, between 26° and 34°, in order to minimize scattering.
(72) Vala, M. T.; Haebig, J.; Rice, S. A. *J. Chem. Phys.* **1965**, *43*, 886−897.
(73) Torkelson, J. M.; Lipsky, S.; Tirrell, M. *Macromolecules* **1981**, *14*, 1601−1603.
(74) Mundra, M. K.; Ellison, C. J.; Rittigstein, P.; Torkelson, J. M. *Eur. Phys. J. Special Top.* **2007**, *141*, 143−151.
(75) We do not use intrinsic fluorescence to measure T_g of the PS domains because the fluorescence signal for ultrathin films is extremely weak, especially for the P(S-*b*-2VP) films where P2VP repeats also absorbs light at the excitation wavelength of phenyl rings.
(76) Gelles, R.; Frank, C. W. *Macromolecules* **1982**, *15*, 1486−1491.
(77) Tsai, F. J.; Torkelson, J. M. *Macromolecules* **1988**, *21*, 1026−1033.
(78) We note that we do not observe any measurable difference in the time scale for self-assembly of a 200 nm thick P(S-*b*-MMA) film, corresponding to 5*L*, and a 220 nm thick film, corresponding to 5.5*L*.
(79) Kalyanasundaram, K.; Thomas, J. K. *J. Am. Chem. Soc.* **1977**, *99*, 2039−2044.
(80) The error bars in Figure 5, nominally ±2 K, represent the uncertainty in our determination of T_g of the PS domains within the block copolymer films. A few of the thinnest films have error bars of ±3 K which reflects the weak contrast of the transition within these films.
(81) We have used ellipsometry in an attempt to observe a second T_g at ∼60 °C, corresponding to that of the 10 nm thick PS surface layer in a 60 nm thick P(S-*b*-MMA) block copolymer film. From the measured temperature dependence of the film thickness, we anticipate three T_gs for the block copolymer film at ∼120 °C for the PMMA domains, at ∼100 °C for the PS middle domain, and at ∼60 °C for the PS surface domain. The transition of the 10 nm thick PS surface domain is expected to be the weakest transition because of its limited contribution to the total film thickness. Our measured ellipsometry results of a 60 nm thick P(S-*b*-MMA) film are suggestive of the presence of these three transitions. However, control measurements of a 60 nm thick PS homopolymer film indicate the presence of a feature (possibly the beta transition [Greiner, R.; Schwarzl, F. R. *Rheol. Acta* **1984**, *23*, 378−395]) in the vicinity of 60 °C, making the conclusive determination of a second T_g at ∼60 °C problematic. We know of no technique that would allow us to isolate better the weak glass transition that is likely occurring in the top 10 nm PS surface domain of the 60 nm thick P(S-*b*-MMA) film.

(82) We obtain the same result even if the bilayer film is annealed at 443 K for 30 min (instead of 418 K for 20 min) prior to the T_g measurement, suggesting that the PS/P2VP interface has reached equilibrium even though the T_g of the P2VP may be significantly increased.

(83) The measurements of Figure 7b,c were made using a pyrene-labeled PS of $M_n = 464\,000$ g/mol and $M_w/M_n = 1.57$ for the top layer and a neat PS of $M_n = 443\,000$ g/mol and $M_w/M_n = 1.27$ for the bottom layer to limit the possibly of the PS layer at the substrate interface dewetting since this trilayer geometry is not energetically favorable. We have found the T_g measurements of the supported multilayer films to be unaffected by molecular weight, consistent with measurements of single-layer PS homopolymer films.[16]

MA070162G